Article No. jmbi.1999.3101 available online at http://www.idealibrary.com on IDEAL® J. Mol. Biol. (1999) 292, 855–869

JMB

Insight into Odorant Perception: The Crystal Structure and Binding Characteristics of Antibody Fragments Directed Against the Musk Odorant Traseolide

Annette C. Langedijk[1], Silvia Spinelli[2], Christelle Anguille[2] Pim Hermans[3], Janny Nederlof[3], Jens Butenandt[4] Annemarie Honegger[1], Christian Cambillau[2]* and Andreas Plückthun[1]*

[1]*Biochemisches Institut Universität Zürich Winterthurerstrasse 190, CH-8057 Zürich, Switzerland*

[2]*Architecture et Fonction des Macromolecules Biologiques UPR 9039, CNRS, IFR1 31 Chemin Joseph Aiguier F-13402, Marseille, France*

[3]*Unilever Research Vlaardingen, Olivier van Noortlaan 120, 3133 AT Vlaardingen, The Netherlands*

[4]*Laboratorium für Organische Chemie, ETH Zentrum Universitätstrasse 16, CH-8092, Zurich, Switzerland*

**Corresponding authors*

Monoclonal antibodies were elicited against the small hydrophobic hapten traseolide, a commercially available musk fragrance. Antibody variable region sequences were found to belong to different sequence groups, and the binding characteristics of the corresponding antibody fragments were investigated. The antibodies M02/01/01 and M02/05/01 are highly homologous and differ in the binding pocket only at position H93. M02/05/01 (H93 Val) binds the hapten traseolide about 75-fold better than M02/01/01 (H93 Ala). A traseolide analog, missing only one methyl group, does not have the characteristic musk odorant fragrance. The antibody M02/05/01 binds this hapten analog about tenfold less tightly than the original traseolide hapten, and mimics the odorant receptor in this respect, while the antibody M02/01/01 does not distinguish between the analog and traseolide. To elucidate the structural basis for the fine specificity of binding, we determined the crystal structure of the Fab fragment of M02/05/01 complexed with the hapten at 2.6 Å resolution. The crystal structure showed that only van der Waals interactions are involved in binding. The somatic Ala H93 Val mutation in M02/05/01 fills up an empty cavity in the binding pocket. This leads to an increase in binding energy and to the ability to discriminate between the hapten traseolide and its derivatives. The structural understanding of odorant specificity in an antibody gives insight in the physical principles on how specificity for such hydrophobic molecules may be achieved.

Keywords: antibody-hapten complex; scFv fragment; CDR-H3; musk odorant; odorant specificity

Introduction

Odorants are usually small hydrophobic, highly volatile molecules which have great importance in the sensory guidance of higher animals and man. Their receptors belong to the large class of G protein-coupled receptors with seven transmembrane helices. These proteins are selectively expressed on the cilia of olfactory neurons in the olfactory epithelium (Schild & Restrepo, 1998; Buck, 1996; Mombaerts, 1996; Buck & Axel, 1991). The odorant receptors have been identified as constituting a large family of homologous receptors (approximately 1000 genes), allowing exquisitely specific interactions of each odorant with a small set of receptors and thus odorant identification in the brain. Very little is known about the structure of the binding sites and, consequently, of the molecular basis of the recognition specificity. The integral transmembrane nature of the receptor makes experimentation very difficult. There are a few

Abbreviations used: CDR, complementarity-determining region; ELISA, enzyme-linked immunosorbent assay; FR, framework, K_D, dissociation constant; KLH, keyhole limpet haemocyanin; NMR, nuclear magnetic resonance; PBS, phosphate-buffered saline; PCR, polymerase chain reaction; PVDF, polyvinyldifluoride; TLC, thin layer chromatography; V_H, variable heavy chain; V_L, variable light chain; OBP, odorant-binding protein; PBP, pheromone-binding protein.

E-mail address of the corresponding authors: cambillau@afmb.cnrs-mrs.fr; plueckthun@biocfebs.unizh.ch

0022-2836/99/390855–15 $30.00/0

reported examples of expression of small amounts of odorant receptors in insect cells (Nekrasova *et al*., 1996; Raming *et al*., 1993) and in bacteria (Kiefer *et al*., 1996), but only recently the functionality of a cloned mammalian receptor has been clearly proven in the rat (Zhao *et al*., 1998).

Small carrier proteins have been shown to exist in insects and mammals, which serve to shuttle odor or pheromone molecules between air and the receptor through the nasal mucus or the sensory lymph (Pelosi, 1994). These proteins are called odorant or pheromone-binding proteins (OBP, PBP). In insects, the PBP/pheromone specificity is very strict, but the three-dimensional structure of these proteins is still unknown. In mammals, OBPs display apparently very little specificity, since they were found to be able to bind any one of tens of different odor molecules with micromolar affinities (Pelosi, 1994). The structure of two OBPs, alone or in complex, have been solved (Tegoni *et al*., 1996; Bianchet *et al*., 1996; Spinelli *et al*., 1998).

Antibodies with narrow specificity may seem an ideal surrogate receptor system, with which many fundamental features of highly specific interactions of such small hydrophobic molecules can be studied, even though the topology of the seven-helix transmembrane protein will almost certainly be entirely different. Furthermore, a surrogate receptor system such as antibodies might have direct biotechnological applications, such as in high-throughput screening for odorants, or as a controlled release system, in which the odorant is given off once the protein is denatured.

To begin to study such questions, we have chosen the musk odorant traseolide (6-acetyl-1-isopropyl-2,3,3,5-tetramethyl-indane) as a model system. Natural musk was first discovered in the exocrine scent glands of the deer-like Moschus animal *Moschus moschiferus,* which lives in the Himalayas. It functions as territorial marker and attracts the female counterpart (Walbaum, 1906; Ohloff, 1990). Since ca 1930, compounds with moschus (musk)-like odor have been synthetically manufactured in large amounts and are used in fragrances for cosmetic and household products (Kevekordes *et al*., 1998).

Here we report the characterization of antibodies against traseolide, their fine specificity against analogs and the structural basis for their specificity as deduced from the crystal structure of a Fab fragment, complexed with traseolide, at 2.6 Å resolution. By expressing a representative member of each family of the anti-traseolide immune response as scFv fragments in *Escherichia coli*, the foundations for further controlled release applications and structure activity relationships can be laid.

Results

Production and screening of cell lines

Mice were immunized with the succinyl derivative of the traseolide hapten, coupled to keyhole limpet haemocyanin (KLH) at position R_1 (Figure 1). Supernatants of stable cell lines were screened in ELISA for the production of monoclonal antibodies recognizing the odor molecule traseolide. Most of the heavy chains were determined to be of subclass IgG1, while light chains were mostly κ-chains.

Antibody variable region sequences

From the panel of antibody-producing cells, eight cell lines were selected for sequence determination of the variable regions. The choice depended on isotype, binding and production levels. The fragments encoding the heavy and light chain variable domains were cloned and sequenced as described in Materials and Methods.

The alignment of the amino acid sequences of the anti-traseolide antibodies reveals that six sequences are highly homologous (<5% differences in V_H and in V_L coding sequences). They are using the same V_κ, J_κ, V_H, D and J_H elements, and were thus most likely derived from the same B-cell. The two other sequences differ considerably in both framework and CDR residues (Figure 2). These two sequences and one member of the group of six were thus chosen for further characterization as scFv fragments (M02/01/01, M02/11/01 and M03/01/01). For convenience the scFv fragments were given shorter names: M02/01/01, scFv Tras-X; M03/01/01, scFv Tras-S (for its serine at position H92; numbering according to Kabat *et al*., 1991); M02/11/01, scFv Tras-L (for its lambda light chain).

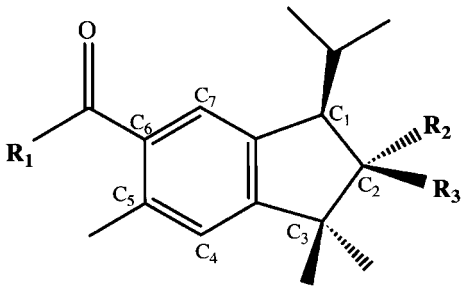

Abbreviation	R_2	R_3	Olfactive description
T^+	CH_3	H	musk
T^-	H	H	odorless
T^{eth}	C_2H_5	H	very weak musk

Figure 1. Traseolide hapten and variants. The structure of the hapten traseolide ((*S*,*S*)-*trans*-6-acetyl-1-isopropyl-2,3,3,5-tetramethyl-indane) ($R_1 = CH_3$, $R_2 = CH_3$, $R_3 = H$) and derivatives in R_2. For immunization, the succinyl derivative of the original musk odorant traseolide was used (T^+, with R_1= HOOC-CH_2-CH_2).

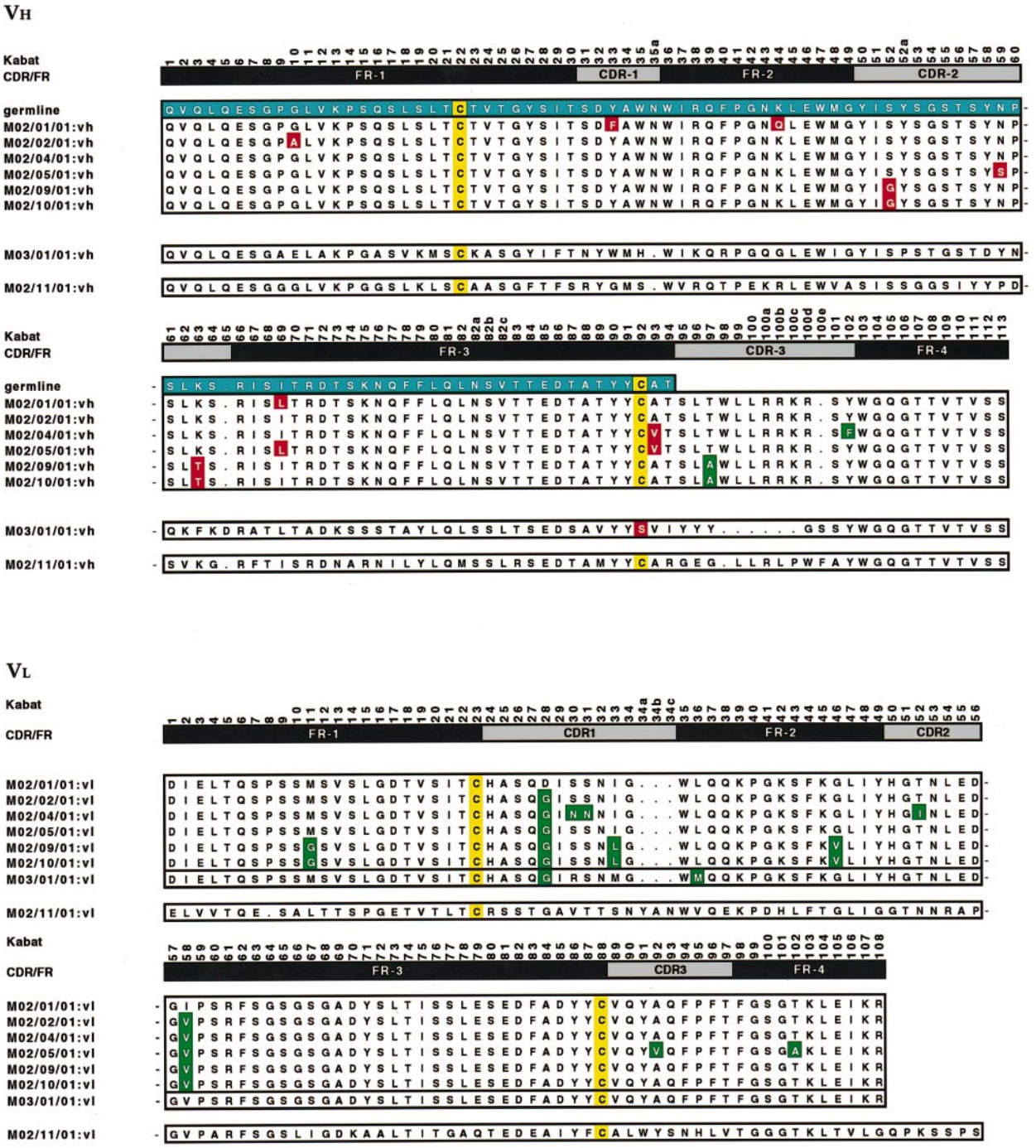

Figure 2. Variable region amino acid sequences of antibodies directed against the hapten traseolide. The germline sequence of the heavy chain of the first sequence group is highlighted in blue (see Materials and Methods). Cysteine residues are highlighted by a yellow background and somatic mutations by a red background. In case no germline sequence was known, sequence deviations from the upper sequence of the sequence group are highlighted by a green background.

The cell line expressing monoclonal antibody M02/05/01 yielded more protein than the cell line expressing the homologous M02/01/01 sequence. Therefore, the M02/05/01 variant was chosen for crystallization as a Fab fragment. The variable regions of the antibodies M02/01/01 and M02/05/01 vary in eight amino acid residue positions (Figure 2). M02/05/01 contains one somatic mutation located in the binding pocket, Ala H93 Val, as became apparent from the X-ray structure of the complex (see below). The germline sequence (Figure 2) has Ala H93, as deduced from sequence statistics with the 40 most closely related antibody sequences of the Kabat database (for details, see

Materials and Methods). The other somatic point mutations do not appear functionally significant, as they are not in the binding pocket and do not directly contact the antigen, but rather simply reflect the background mutation rate.

Expression, isolation and detection of scFv fragments

The V_H and V_L genes were cloned in scFv format (V_H-linker-V_L) with a N-terminal FLAG-tag and a C-terminal Myc and His-tag in the vector pIG6 (Ge *et al.*, 1995). The scFv fragments were expressed in the periplasm of *E. coli*. In the soluble, periplasmic fraction scFv Tras-S (from the mAb M03/01/01) and scFv Tras-L (from the mAb M02/11/01) were detected in reasonable amounts (ca 1 mg/l *E. coli*), while only a small amount of scFv Tras-X (from the mAb M02/01/01) was found (Figure 3(a)). In the insoluble fraction a double band for scFv Tras-X was observed (data not shown; cf. Figure 3(b)).

Examination of the amino acid sequence of scFv Tras-X showed a rare sequence of four positively charged residues in CDR3 of the heavy chain. To check whether these residues were causing the problems in the periplasmic production of the fragment, two mutations were introduced to give the mutant Tras-P, which substituted the charged residues by neutral amino acids: Arg H100a Leu and Lys H100c Gln. These residues were selected with the help of a preliminary model structure of the antibody variable fragment, applying the criterion that the backbone conformation of CDRH3 would stay intact (A. van Beusekom, data not shown). The subsequently obtained crystal structure (see below) showed this assumption to be correct. The CDRH3 mutations indeed led to a much higher yield of soluble scFv in the periplasm (Figure 3(a), mutant Tras-P *versus* Tras-X).

On a Western blot developed with antibodies recognizing a C-terminal His-tag, the insoluble fraction of the scFv Tras-X shows a double band (Figure 3(b)). One band has the identical molecular mass as mutant scFv Tras-P, presumably the correctly processed scFv protein, while the second band has a slightly higher molecular mass. Only the lower one is detected in the Western blot developed with antibodies recognizing the N-terminal FLAG sequence (Figure 3(c)). This means that the FLAG sequence is not at the N terminus in the upper band (Knappik & Plückthun, 1994), and is therefore not recognized by this anti-FLAG antibody, but Tras-X must carry an N-terminal extension, most likely the signal sequence. Positive charges have been observed before to interfere with transport through the membrane (Ayala *et al.*, 1995; Summers *et al.*, 1989; von Heijne, 1986). Thus, the removal of two positive charges in CDRH3 (to interrupt the positive charge cluster) improved the amount of periplasmic protein, presumably at least in part because of more efficient membrane transport. Additionally, the positively charged cluster may have provided a protease target (Volkin & Klibanov, 1989; Hammarberg *et al.*, 1990) and thus the mutations may have stabilized the protein, once it is in the periplasm.

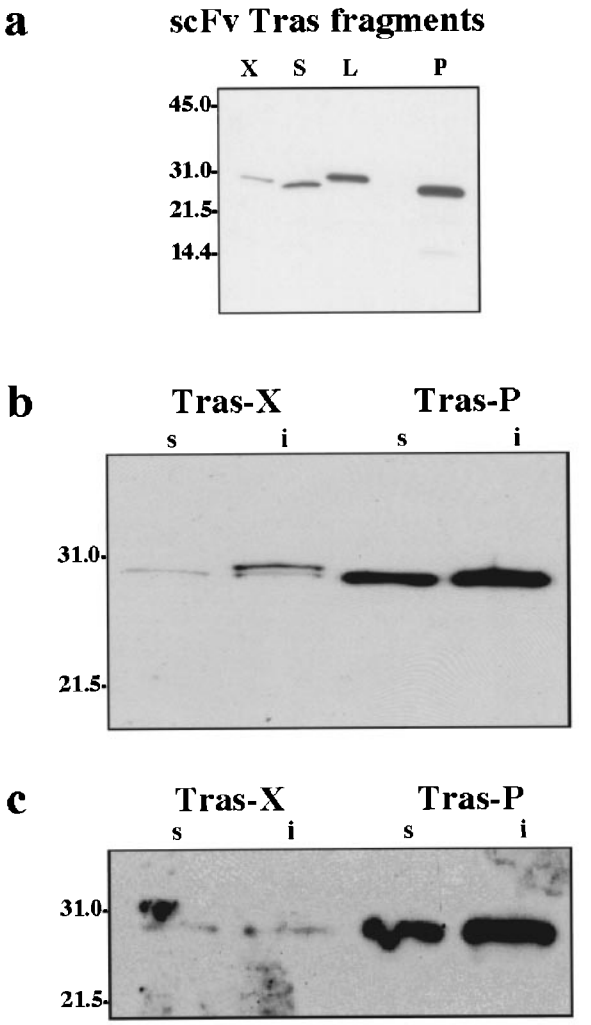

Figure 3. (a) Western blot of the soluble periplasmic fraction of scFv Tras fragments. The Western blot was developed with an anti-His tag antibody as the first antibody. Western blots of scFv Tras-X and mutant scFv Tras-P developed with either (b) an antibody against the C-terminal His tag, or (c) an antibody against the short N-terminal FLAG. The soluble and insoluble periplasmic fractions are labeled s and i, respectively. The positions of the molecular mass markers (in kDa) are indicated on the left.

The functionality of the scFv Tras-P, Tras-L and Tras-S fragments was checked qualitatively by an inhibition ELISA assay. Equal amounts of soluble periplasmic fractions were applied to microtiter plates coated with the traseolide antigen, and the inhibition by soluble traseolide was determined. All showed specific ELISA signals of the same order of magnitude (data not shown). To quantitatively investigate the effect of the CDRH3 mutations on the binding properties of

the antibody fragment, the K_D values of scFv Tras-X and the mutant Tras-P were determined by fluorescence titration. Both fragments were produced as cytoplasmic inclusion bodies in *E. coli*, refolded and purified by affinity chromatography with the hapten traseolide. Using this method, the positive charges could not affect the expression of the scFv fragment. The binding constant was determined by a direct fit of the protein fluorescence signal as a function of the hapten concentration (Jung & Plückthun, 1997). The scFv Tras-X has a K_D of 2.0×10^{-7} M and the scFv Tras-P a K_D of 3.5×10^{-7} M, which is within the range of error and also not significantly different from the parent antibody (see below).

Binding assays: competition BIAcore and fluorescence titration

Fluorescence titration of M02/05/01 and M02/01/01

Fluorescence titration experiments were performed with the mAb and the scFv Tras-X fragment of M02/01/01 and the mAb and Fab fragments of M02/05/01. M02/05/01 is the antibody for which the X-ray structure of the Fab fragment was determined (see below), and M02/01/01 is closely related, but carries the germline amino acid Ala H93 in the binding pocket. The binding specificity of the antibodies M02/05/01(Val H93) and M02/01/01(Ala H93) was investigated quantitatively by determining the binding constants of three structurally related traseolide variants. The traseolide variants used were the succinyl derivatives of T^+, T^- and T^{eth} (Figure 1).

The comparison of the binding characteristics of the two related antibodies M02/05/01 and M02/01/01 showed that the binding to the original hapten differs significantly: the K_D of the antibody M02/05/01 (Val H93) is 2.7×10^{-9} M, while the antibody M02/01/01 (Ala H93) shows a K_D of 1.6×10^{-7} M for the same hapten, which corresponds to a difference in dissociation constant of a factor of ca 75 (Table 1). Another remarkable finding is that for M02/01/01 (Ala H93) no significant differences were found in binding constant between the three closely related traseolide variants. For M02/05/01 (Val H93), however, the odorless variant T^-, lacking one methyl group (Figure 1), showed a tenfold lower affinity than the original T^+ hapten. The T^{eth} variant, which has an ethyl group instead of a methyl group at this position (Figure 1), bound with about the same affinity as the original hapten T^+. As expected, the Fab fragment of M02/05/01 and the recombinant scFv Tras-X (from M02/01/01) fragment have very similar binding behavior as their parent mAb to monomeric soluble hapten, and the small differences may indicate the limits of the accuracy of the measurements.

BIAcore measurements of M02/11/01 and M03/01/01

Purified monoclonal antibodies M02/11/01 and M03/01/01 (the parent mAbs of scFv Tras-L and Tras-S) were used for K_D determination in solution by competition BIAcore analysis (Karlsson, 1994; Nieba *et al.*, 1996; Hanes *et al.*, 1998). In this experiment, the monoclonal antibody was incubated with the soluble succinyl derivative of traseolide, and the mixture was injected on a BIAcore chip containing immobilized BSA-traseolide conjugate at high density. Only free antibody, but not hapten-bound antibody, can bind to hapten on the surface, analogous to the Friguet-Goldberg ELISA (Friguet *et al.*, 1985). The observed mass-transfer limited rates therefore indicated the amount of free antibody in solution as a function of hapten concentration. In this way, the correct dissociation constant in solution could be obtained, independent of any BIAcore rebinding errors (Schuck, 1997). The slopes of the BIAcore signal, which correspond to the initial binding rates (k_{obs}), were plotted against the corresponding total hapten concentration, and fitted to determine the dissociation constant (Hanes *et al.*, 1998). The K_D of M02/11/01 was calculated as 2.1×10^{-9} M and that of M03/01/01 as 1.8×10^{-8} M (Table 1).

Table 1. Determination of the dissociation constants of anti-traseolide antibodies with structurally related antigen variants

	T^+		T^-		T^{eth}	
Antibody	K_D (M)	ΔG (kcal/mol)	K_D (M)	ΔG (kcal/mol)	K_D (M)	ΔG (kcal/mol)
mAb M02/05/01[a]	2.7×10^{-9}	−11.4	1.5×10^{-8}	−10.4	2.8×10^{-9}	−11.4
Fab M02/05/01	1.9×10^{-9}	−11.6	1.9×10^{-8}	−10.3	2.0×10^{-9}	−11.6
mAb M02/01/01[a]	1.6×10^{-7}	−9.1	ND	ND	1.4×10^{-7}	−9.2
scFv Tras-X	2.0×10^{-7}	−8.9	3.5×10^{-7}	−8.6	3.2×10^{-7}	−8.8
mAb M02/11/01	2.1×10^{-9}	−11.5	ND	ND	ND	ND
mAb M03/01/01	1.8×10^{-8}	−10.3	ND	ND	ND	ND

The dissociation constants were determined by following the fluorescence emission at a constant wavelength (334 nm) as a function of antigen concentration (mAb M02/05/01 and mAb M02/01/01), or by mass-transport limited competition BIAcore (mAb M02/11/01 and mAb M03/01/01). Subsequently, the data were fitted to a quadratic function (see Materials and Methods).

[a] M02/05/01 carries Val H93 in the variable domain, while M02/01/01 carries Ala H93.

X-ray structure of bound and unbound Fab M02/05/01

The three-dimensional structures of Fab M02/05/01 complexed with the succinyl derivative of the traseolide hapten was solved at 2.6 Å resolution. The quality of the Fab-hapten structure can be estimated from the diffraction and refinement data (Table 2), from the electron density map (Figure 4) and from the Ramachandran plot, in which 85 % of the residues are located in the most favorable areas (data not shown). The ''elbow'' angle, made by the pseudo-2-fold axes relating V_H to V_L and C_{H1} to C_L is ~169°, giving an elongated Fab structure with few intra-chain, interdomain contacts. A total of 120 water molecules were fitted to the Fab-hapten model.

The electron density for the predominantly bound (*S*,*S*)-traseolide is of high quality, making it possible to position it with good precision (Figure 4). We cannot exclude the presence of some minor fraction of (*R*,*R*)-traseolide in the binding site. At a contour level of 1.2σ all hapten atoms are associated with electron density. Accordingly, the *B*-factors of 25.0 Å^2 for the hapten are relatively low compared to the average (40.5 Å^2; Table 2).

The variable domains have very long complementarity-determing regions (CDRs), especially H3 and L1, which protrude from the combining site and form a very deep cleft between each other (Figure 5). The long CDRH3 runs in the middle of the cleft and folds back, forming a flat floor for the combining site. The traseolide hapten is located in a deep hydrophobic pocket (Figure 6) involving part of the β-sheets and both CDR3 of the heavy and light chain (H3 and L3) (Figure 5 and Table 3). The binding pocket is approximately 12 Å deep and 7 Å wide, which is sufficient to bury in the complex 450 Å^2 of the water-accessible surface area of traseolide (of 531 Å^2 in total) (Figure 6). As expected for a hydrophobic hapten, the nature of the combining site is hydrophobic (Figure 7 and Table 3). The hydrophobic ring system is contained in the cavity, while the succinyl moiety is directed towards the solvent and is hydrogen-bonded to two water molecules, W42 and W52, located at 2.5 Å and 3.9 Å, respectively (Figure 7). The majority of aromatic residues are found within 6 Å of the hapten: Trp H47, Tyr H50, Trp H103 from the heavy chain, and Tyr L49, Tyr L91, Phe L94, Phe L96, Phe L98 from the light chain. A few aliphatic (Ile H37, Val H93, Leu H96, Leu L36 and Val L89) and polar non-charged amino acid residues (Asn H35a, Thr H94, Ser H95, Ser H101 and Gly L34) complete the active site (Figure 7). Two charged residues are found in the vicinity of the hapten. Lys H100c is located at 4.5 Å from the carboxylate of the succinyl moiety, while Glu L55 is located on a side of the cavity, at 4.8 Å from one of the methyl group of the isopropyl motif of the hapten. This is not a close distance, however, and the charge of Glu L55 is compensated by Arg

Table 2. Data collection and final refinement statistics

A. *Data collection*	
Resolution limit (Å)	20.0-2.6
Data completion (I/σ[*I*] > *I*; (all/last shell)	88.0/55
Redundancy	5
R_{sym} (all/last shell)[a]	13./30.
B. *Refinement*	
Resolution limit (Å)	12.00-2.6
Number of reflections	15,749
Number of protein atoms	3347
Final *R*-factor/R_{free}[b]	20.5/27.0
B-factors:main/side-chain-solvent (Å^2):	32/33.5-44.0
r.m.s. deviations from ideal values:	
Bonds (Å)/angles (deg.)	0.010/1.65
Improper/dihedral angles (deg,)	2.5/28.5
Estimated error (Luzzati plot) (Å)	0.18

[a] $R_{sym} = \Sigma\ (\Sigma|I(h)i - \langle I(h)\rangle|/\Sigma\langle I(h)\rangle)/n$; $I(h)i$ is the observed intensity of the *i*th measurement of reflection *h*, and $\langle I(h)\rangle$ the mean intensity of reflection *h*.
Last shell: 2.6-2.7 Å.
[b] $R = \Sigma|F_o - F_c|/\Sigma[F_o]$; F_o and F_c are the observed and calculated structure factor amplitude, respectively.

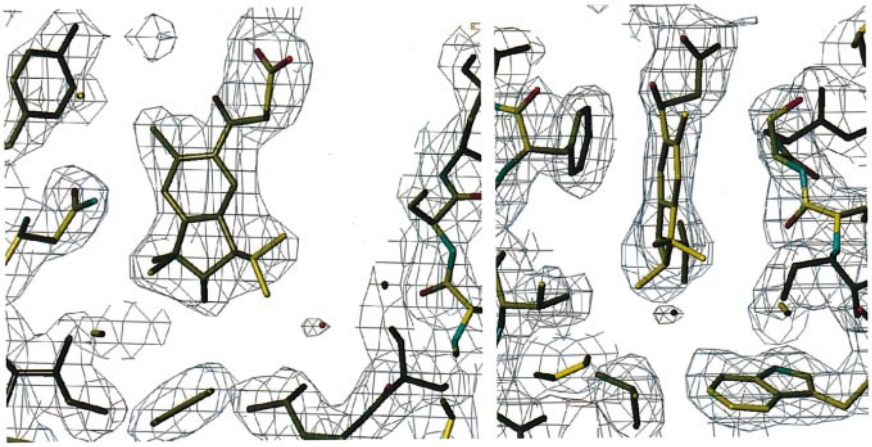

Figure 4. Views (90°) of the electron density map contoured at 1 sigma around the traseolide molecule and the combining site.

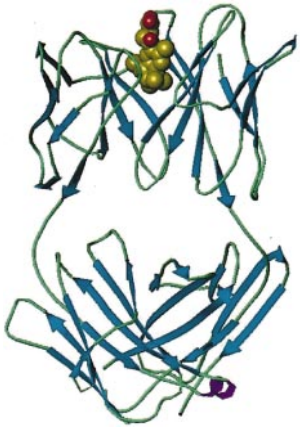

Figure 5. Schematic view of the Fab C^{α} secondary structure trace and the bound traseolide molecule (in CPK, C yellow, O red). The β-strands are displayed as blue arrows. Note the interaction of the traseolide molecule with the β-strands, belonging to the framework.

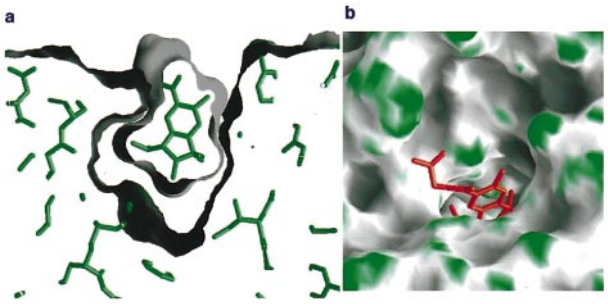

Figure 6. The molecular surface of the Fab fragment at the combining site and of the hapten. (a) View of a molecular slice of the complex, emphasizing the non-perfect complementarity of the surfaces. (b) Orientation of the traseolide molecule in the combining site groove. The surface is colored according to the curvature.

H100d and Lys L45. The shape of the cavity is not fully complementary to that of the ligand. There is enough room for larger substituents of the cyclopentane ring.

Discussion

Variability in antibodies directed to a small hapten

The alignment of the amino acid sequences of the variable domains of the anti-traseolide antibodies (Figure 2) showed that antibodies of three types were obtained. A group of six antibodies, derived from Kabat subgroup V_HIB, and V_κII, M02/11/01 derived from V_HIB, and V_λ and M03/01/01 derived from V_HIIB and V_κII. The heavy chain of M03/01/01 contains a very peculiar mutation, the highly conserved Cys H92 is substituted for a Ser residue, and thus the disulfide bridge in the heavy chain of this variable domain cannot be formed. The consequences for stability have been investigated in detail elsewhere (Langedijk *et al.*, 1998).

The sequence diversification by somatic mutations has been studied in several anti-hapten systems. It has been reported that mAbs produced against small ligands such as arsonate (Wysocki *et al.*, 1987), morphine (Kussie *et al.*, 1989), cyclosporine (Schmitter *et al.*, 1990), oxazolone (Solin *et al.*, 1992) and progesterone (Arevalo *et al.*, 1993) tend to show a high degree of restriction in the germline V-region gene usage. In contrast, the antibodies raised against the small hapten traseolide show some diversity in the heavy and light chain subclasses used. Also for dioxin (Recinos *et al.*, 1994) and for *N*-(*p*-cyanophenyl)-*N*′-(diphenylmethyl)guanidineacetic acid, a high potency sweetener (Anchin & Linthicum, 1993), diverse structural solutions for the recognition problem of a small molecule were noted. Thus, for small compounds both restricted and diverse immune response have been found.

The dissociation constants of the antibodies from the different sequence groups to the traseolide hapten were determined, using either fluorescence titration or competition BIAcore (Table 1). Although small differences in experimental parameters like pH and temperature will always be present, the data may be compared because both methods are based on measurements in solution (Nieba *et al.*, 1996). M02/05/01 and M02/11/01

Table 3. Fab residues in contact with the hapten

Position	Amino acid and atom	Segment	Shortest contact (Å)
L91	Tyr CD1	CDR3	3.4
L96	Phe CE1	CDR3	3.5
H35a	Asn CD1	CDR1	3.5
H47	Trp CD1	FR2	3.7
H50	Tyr CE1	CDR2	3.8
H93	Val CG2	FR3	3.6
H95	Ser CB	CDR3	3.9
H96	Leu CD2	CDR3	3.3

Cutoff is 4.0 Å.

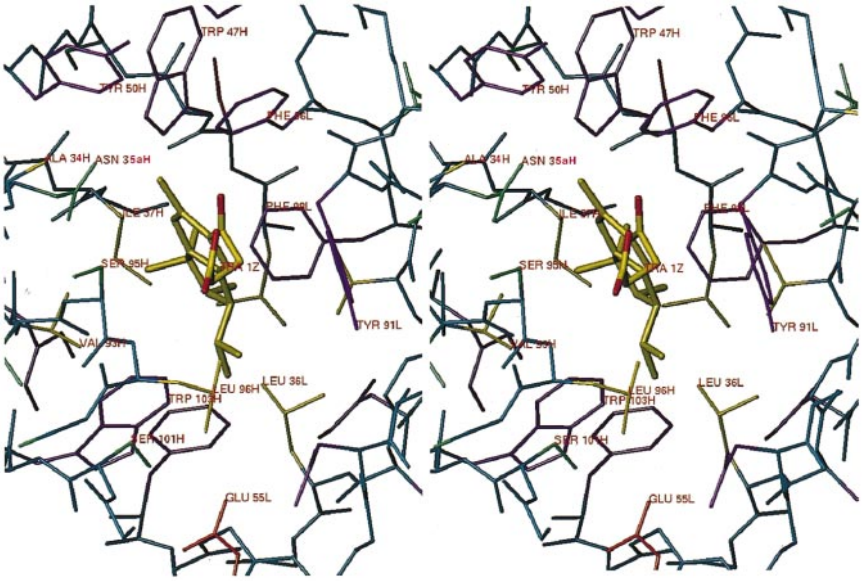

Figure 7. Stereoview of the traseolide hapten in the combining site. Heavy and light chain backbones are blue and pink, respectively. Side-chains of aromatics are magenta, aliphatics are yellow, polar non-charged are light green, basic residues are light blue, and acidic residues are red. Fab residues in contact with the hapten within 4 Å are: Asn H35a, Trp H47, Tyr H50, Val H93, Ser H95, Leu H96, Tyr L91 and Phe L96; with a distance between 4-6 Å: Ile H37, Thr H94, Lys H100c, Ser H101 and Trp H103, and Gly L34, Leu L36, Tyr L49, Glu L55, Val L89, Phe L94 and Phe L98.

bind to the hapten with similar free energy, while M02/01/01 and M03/01/01 have dissociation constants that are one to two orders of magnitude higher.

Binding sites for small hydrophobic ligands

There are two driving forces to antigen binding: entropic forces by the hydrophobic effect (liberation of water molecules from apolar protein surfaces upon complex formation) and enthalpic forces (Mariuzza *et al*., 1994). Antibodies, even directed to the same target, differ greatly in the relative contribution of each component, and no general rules can be drawn (Malby *et al*., 1994). In general, the specificity of antibodies is dependent on the precise nature of the binding surface and the presence or absence of hydrogen bonds and charge-charge interactions.

Binding of small hydrophobic haptens to antibodies usually occurs deep in the hydrophobic cleft of the antibody, and thus involves framework residues. Specificity is generally achieved by involving charged residues and hydrogen-bond interactions (Webster *et al*., 1994), e.g. steroid hormones (Trinh *et al*., 1997; Arevalo *et al*., 1994) or fluorescein (Omelyanenko *et al*., 1993). There are, however, also examples of specific binding devoid of these polar group interactions. The high affinity binding of antibody 26-10 for digoxin is solely derived from shape complementarity (Jeffrey *et al*., 1993). The traseolide hapten is also a small hydrophobic molecule, and binding is almost entirely due to van der Waals forces and the hydrophobic effect. Both the keto moiety and the carboxylate terminus of traseolide do not seem to have possibilities for hydrogen bonding in close vicinity, since Lys H100c, the closest charge, is found at 4.5 Å from the carboxylate group of traseolide (Table 3). This was expected for the carboxylate moiety, because during immunization it was not freely accessible, but coupled to KLH.

Binding specificity: affinity for related hapten variants

From the crystal structure of Fab M02/05/01, the fit of the hapten-antibody contacting surface seems remarkably good. The traseolide hapten has been found in a deep hydrophobic pocket lined with many aromatic residues (Figures 6 and 7). However, there are some imperfections in that cavities remain in the complex. The side of the binding pocket fits well with the hapten, while the bottom of it is not that close to the molecular surface of the hapten.

Visual inspection of the crystal structure showed that different musk molecules could be fitted as well. Substituting ethyl for methyl in the R_2 position (Figure 1) results in slightly better contacts with Leu L36 and Trp H103. Substituting a methyl group by an hydrogen atom in R_2, however, might be unfavorable, as a cavity would be generated unless the van der Waals contact is maintained by rotation of the whole hapten. These findings fit well with the experimental data (Table 1).

Filling up a stable empty cavity in the binding pocket by the ligand might be a general strategy to

improve binding energy. An additional 4-methyl group attached to the piperidine ring of 3-amidinophenylalanine-derived inhibitors to thrombin gave rise to a 17-fold better binding (Bergner *et al.*, 1995). The more complete spatial occupancy of the hydrophobic S2 cavity probably accounts for an increase in free binding energy by 1.5 kcal/mol. Recently, Dougan *et al.* (1998) attempted to increase the binding affinity of the scFv antibody NC10 for its anti-influenza virus antigen. A cavity in the binding interface was filled with a larger antibody side-chain. However, the replacement of Leu L94 with Tyr or Trp abolished binding, while a valine residue led to a reduction in Gibbs free energy ($\Delta\Delta G = 0.9$ kcal/mol). The cavity creating mutation Leu L94 Ala abolished binding completely.

Effects of somatic mutations in M02/05/01

The variable regions of the monoclonal antibodies M02/01/01 and M02/05/01 vary in eight amino acid positions. M02/05/01 contains one somatic mutation that makes direct van der Waals contact to the traseolide hapten: Ala H93 Val. Apart from an about 75-fold improved binding energy of M02/05/01 compared to M02/01/01 for traseolide, the antibody shows also an increased binding specificity as it discriminates traseolide better from its non-smelling derivative (Table 1). Although it cannot be excluded that the other somatic mutations contribute to the altered binding characteristics of M02/05/01, the Ala H93 Val mutation is the one most likely to be responsible.

The presence of Ala H93 in M02/01/01 will enlarge the cavity compared to the Val H93 in the structure of M02/05/01 solved here. This may explain the difference in fine-specificity for traseolide variants: M02/05/01 (Val H93) has a slightly higher affinity for T^{eth} then for T^+, while T^- binds considerably less well (by 1.2(±0.1) kcal/mol; Table 1). For M02/01/01 (Ala H93) no substantial differences in binding affinity were found between the three traseolide variants (Table 1). By filling an existing cavity Val H93 provides a tighter association to the traseolide hapten, leading to better binding affinities and fine specificity for traseolide variants (Figure 8). This binding energy is lost by creating a cavity, either by removing the side-chain of Val H93, or by removing the methyl group on C_2 of traseolide. This illustrates how increase in binding energy is coupled to specificity.

The importance of FR3 residue H93 was described before for V_HOx1 antibodies, where Ala H93 plays a critical role in the formation of the hydrophobic phOx binding pocket (Alzari *et al.*, 1990). In the Brookhaven database (http://www.rcsb.org/pdb/) very few structures are found in which H93 makes contact to the antigen: the catalytic antibodies 1eap and 1kno and the fluorescein binding Fab fragment 4fab. As residue H93 is located deep in the binding pocket, only small haptens are able to make contact to it.

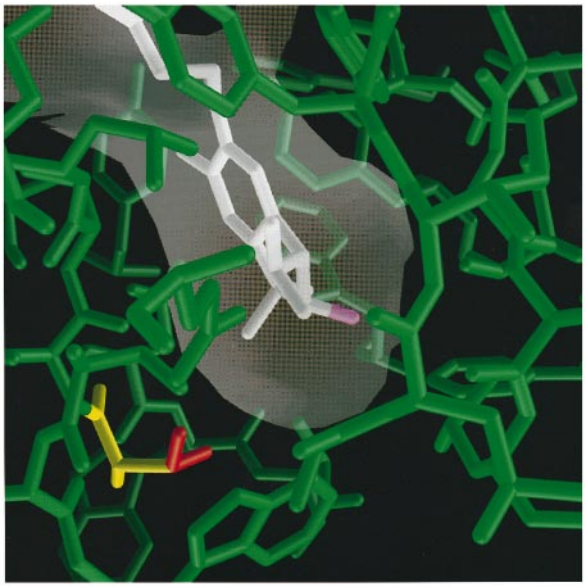

Figure 8. The binding pocket of the crystal structure of the complexed Fab M02/05/01. The antibody residues are given in green, the hapten in white. Residue H93 of the Fab fragment is highlighted (Val H93 in red and germline Ala H93 in yellow), as well as the C_2 methyl-group of the hapten (the C_2 methyl-group in cyan). The Connolly surface of the antibody binding pocket is shown as a transparent surface.

The increase in binding due to the somatic Ala-Val mutation in the binding pocket of M02/05/01 corresponds to an increase in free energy of 2.3 kcal/mol (Table 1). This value is in the range that is generally observed for such a change. Studies on enzyme-substrate interactions have shown that the contribution of hydrophobic groups to binding can be large and variable, up to 3.5 kcal/mol per methylene group (Fersht, 1985). For comparison, the contribution of a buried methylene group to protein stability was found to depend on its local environment and averages ca 1.5(±0.6) kcal/mol (Serrano *et al.*, 1992; Jackson *et al.*, 1993), and this can be a decisive contribution to the free energy of folding, which is generally quite small, typically 5-15 kcal/mol (Privalov, 1979). Bode (1979) measured the difference in free-energy for the binding of dipeptides to *p*-guanidinobenzoate-trypsinogen. Upon substituting a Val for an Ala in the dipeptide (and leaving the second residue identical) an increase of 2.9-3.1 kcal/mol in binding energy was found.

Force-field calculations were performed to rationalize the experimentally observed differences in ligand binding energies of the closely related antibodies M02/01/01 (Ala H93) and M02/05/01 (Val H93), and to provide a microscopic description of the processes involved. The binding energies of M02/05/01 (Val H93) and M02/01/01 (Ala H93) to the traseolide variants T^+ and T^- were calculated using the TAFF force-field (Clark *et al.*,

1989) after energy minimization of the complex. The inter-molecular van der Waals energy showed the same trend as the experimental data, underlining the importance of the surface complementarity. However, the absolute binding energies were not predictive, probably due to the approximate method used (M. Scarsi, unpublished data).

Receptor mimicry

The molecular basis for the mimicry between antibodies and receptors has been questioned; the observation that two proteins recognize the same ligand does not imply that they share common structure in their binding sites (Ámati *et al*., 1995; Ducancel *et al*., 1996). Nevertheless, the working concept of using mAbs as ''surrogate receptors'' has proved useful in the discovery of lead compounds for pharmaceutical and related purposes, because antibodies raised against receptor-specific ligands share binding properties with the receptors (Cook & Drayer, 1988; Döring *et al*., 1994). The binding specificity profile of monoclonal antibody NC6.8 appears to correlate with the sweetness potencies of the superpotent sweetener ligand (Anchin *et al*., 1997), and the antibody 1B7 raised against the β-adrenergic receptor ligand alprenolol demonstrated high affinity and stereoselectivity for both β-adrenergic agonists and antagonists, which makes it an ideal model of the receptor's binding site (Sawutz *et al*., 1985).

Also, the Tras antibodies may exhibit some chemical and structural interaction motifs as found in the natural biological odorant receptor. For the monoclonal antibody M02/05/01 used in this study it was found that musk odorant T^+ binds better than the odorless T^- (Table 1). From the crystal structure of Fab M02/05/01 it is clear that a methyl group connected to the indane ring of traseolide will give a better shape complementarity. The affinity for T^{eth} (very weak musk) seems to correlate less well with the olfactive description and is antibody dependent: M02/05/01 bound T^{eth} and T^+ in a comparabe manner.

To be able to distinguish such an enormous variability of odorants, we predict that the ligand would have to fit very precisely to the odorant receptor. If they leave a cavity, the specificity would be lost. In analogy to the traseolide binding pocket odorant molecules might bind deeply in a binding pocket, between adjacent trans-membrane helices, but probably also contacting the loops connecting the helices. Very recently more evidence for this hypothesis was found by Krautwurst *et al*. (1998). They expressed full-length odorant receptors in HEK-293 cells and found that the mouse 17 receptor, unlike the highly homologous rat 17 receptor, prefers heptanal instead of octanal. Both receptors differ by a single valine to isoleucine substitution in transmembrane region V of the odorant receptor. In addition, the preservation of complementarity between the receptor and the ligand seems to play a key role in odorant recognition.

Conclusions

A small hapten like the musk odorant traseolide is able to create an antibody response of significant sequence diversity in the mouse. Obviously, binding of an odorant to a protein can occur in different binding modes.

Fine specificity of a monoclonal antibody for the musk odorant traseolide is regulated primarily by shape complementarity and the concomitant desolvation of the complementary surfaces; there are no apparent energetic contributions from ionic or hydrogen-bonding interactions.

The increase in binding energy is coupled to an increase in specificity: a single somatic mutation in the binding pocket of M02/05/01 led to a considerably better binding of the traseolide hapten ($\Delta\Delta G = -2.3(\pm 0.1)$ kcal/mol). At the same time the Ala-Val mutation caused more specificity for hapten variants: the non-smelling traseolide odorant lacking a methyl group was binding about a factor 10 less tightly than the original traseolide.

Materials and Methods

Materials and strains

For all cloning experiments the *E. coli* K12 strain JM83 (λ^-, *ara*, Δ(*lac*, *pro*AB), *rpsL*, *thi*, ϕ80, *dlac*ZΔM15) (Yanisch-Perron *et al*., 1985) was used. The scFv proteins were expressed as soluble proteins in the periplasm in the *E. coli* strain JM83, or as cytoplasmic inclusion bodies in the *E. coli* strain BL21(DE3) (F^-, *ompT*$^-$, $r_B^- r_B^-$, (λimm21, *lac*I, *lac*UV5, T7pol, *int*)) with the T7 polymerase-based system (Studier & Moffatt, 1986).

Immunization, fusion and subcloning

The commercial musk odorant traseolide (Quest International, the Netherlands) was used as hapten (Figure 1). Immunization, production of monoclonal antibodies, screening for hapten specificity, mRNA isolation and subcloning was performed as described (Langedijk *et al*., 1998).

Antibody germline determinations

The 40 sequences of the Kabat database (http://immuno.bme.nwu.edu) most closely related to the heavy or light chain sequence of interest were aligned with the ''FASTA'' option of the GCG package (Genetics Computer Group, 1991; Markiewcz, 1991). The data were aligned with ''PILEUP'' and reformatted with the ''PRETTY'' command, using the same package. Subsequently the data were imported in an Excel macro, to highlight deviations from the consensus sequence (developed by A. Honegger). A prerequisite for the analysis is that the database contains enough sequences of the germline corresponding to the input sequence. For the heavy chain of M02/05/01 the germline consensus sequence could be determined, because 24 sequences of the same germline were present in the database. The light chain of M02/05/01, however, could not be classified, because no sequences of antibodies with the same germline were found (data not shown).

Construction of plasmids

The V_H-$(Gly_4Ser)_3$-V_L construct was obtained by cloning V_H and V_L in the vector pHJ300 (Knappik & Plückthun, 1994). Overlap-PCR was used for subcloning the scFv gene in the vector containing N-terminal FLAG and C-terminal Myc and His-tags. The overlap was used to introduce a N-terminal *Eco*RV site and a C-terminal *Eco*RI site, corresponding to the vectors used. For periplasmic expression the gene was subcloned in pIG6 (Ge *et al*., 1995) and for cytoplasmic expression, the gene was subcloned in pTFT74 (Freund *et al*., 1993; Ge *et al*., 1995) which places expression under control of the T7 promoter.

The mutant antibody fragment Tras-P was constructed by site-directed mutagenesis using PCR with primers containing the desired mutation. After sequencing the mutated part, the gene was digested and ligated in the original plasmid.

Periplasmic scFv expression and fractionation

LB medium (25 ml) containing 100 μg/ml ampicillin was inoculated with an *E. coli* overnight culture harboring the plasmid encoding the respective antibody fragment. Cultures were incubated at room temperature (RT, 25 °C) until an A_{600} of 0.5 was reached. Then IPTG (isopropyl β-D-thiogalactopyranoside) was added to a final concentration of 0.5 mM and the incubation was continued for three hours. After induction, aliquots of the cell cultures (with an equal amount of *E. coli* cells as calculated according to the A_{600}-value, usually 20 *A* units) were removed, and the cells were fractionated with an osmotic shock according to a modification of the procedure by Witholt *et al*. (1976). After centrifuging the cells at 4500 rpm for ten minutes, the cell pellet was resuspended in 0.5 ml spheroplast buffer (200 mM Tris-HCl, 0.5 mM EDTA, 0.5 M sucrose, pH 8.0) at 4 °C. The suspension was gently mixed, incubated for 30 minutes on ice and centrifuged for ten minutes at 4500 rpm at 4 °C. The pellet was resuspended in the same volume as the spheroplasts, 0.5 ml of mM $MgCl_2$, and incubated on ice for another 30 minutes and centrifuged as above. Both supernatant fractions were pooled as the soluble periplasmic fraction, whereas the pellet was dissolved in 1 ml PBS.

Cytoplasmic scFv expression

Inclusion body protein was produced as described and was isolated following a standard protocol (Buchner & Rudolph, 1991; Langedijk *et al*., 1998). Purification of inclusion body protein and refolding were carried out as described by Proba *et al*. (1997), except that the formation of disulfide bonds was allowed by the presence of both 0.5 mM of reduced and 0.5 mM oxidized glutathione in the refolding buffer. After incubation of one to four days at 4 °C the refolding mixture was applied to a hapten-affinity column.

Hapten-affinity chromatography

Refolded, functional protein was purified using affinity chromatography with non-specific elution with acidic buffer (100 mM glycine, pH 2.7) and immediate neutralization with one-quarter volume of 1 M Tris (pH 8.0) (Langedijk *et al*., 1998). Purity of the protein was controlled by Coomassie-stained SDS-PAGE. If necessary the purified scFv was concentrated by centrifugal filtration with an Ultrafree concentrator (Millipore). Yields were calculated by absorption at 280 nm, using calculated extinction coefficients (Gill & von Hippel, 1989).

Protein-gel electrophoresis and Western blots

The antibody fragments were detected by reducing SDS-PAGE (Laemmli, 1970) and subsequent Coomassie staining or Western blotting. For periplasmically expressed proteins, the samples were normalized to the amount of cells.

Polyacrylamide gels were blotted on PVDF membrane (Immobilon-*P*, Millipore; Tovay & Baldo, 1987) and after blotting the gel was immuno-stained using the anti-FLAG antibody M1 (Kodak) (Prickett *et al*., 1989), or the anti-His tag antibody (Lindner *et al*., 1997) as the first antibody, and then an Fc-specific goat anti-mouse antiserum conjugated to horseradish peroxidase (HRP) as second antibody (Pierce). Luminescence was detected with the ECL™ kit (Amersham), or color was developed with BM-blue peroxidase precipitating substrate (Boehringer Mannheim).

BIAcore measurements

Competition BIAcore analysis was performed under mass-transport limitation as described (Karlsson, 1994; Nieba *et al*., 1996), using a sensor chip CM5 (Pharmacia) coated with 10,000 RU of BSA-traseolide conjugate or with only BSA as a control. Immobilization of BSA was performed as follows: 35 μl of a 1:1 mixture of 0.1 M *N*-hydroxysuccinimide (NHS, Fluka) and 0.2 M *N*-(3-dimethylaminopropyl)-*N*′-ethylcarbodiimide hydrochloride (EDC, Fluka) was pumped across the chip to activate the carboxmethylated dextran surface. Subsequently 30 μl of 3 μM BSA-traseolide (or BSA) solubilized in NH_4Ac (pH 4.5) was pumped across the activated surface. After coating sufficient protein (which was followed by the increasing resonance units) the residual NHS esters were inactivated with ethanolamine. Each binding-regeneration cycle was performed with a constant flow rate of 20 μl/minute using 20 mM Hepes (pH 7.6), 150 mM NaCl, 0.005 % (v/v) Tween-20 (HBST). Samples of 200 (μl of antibody in HBST, containing various amounts of succinyl derivatives of the traseolide hapten and preincubated for at least one hour at 4 °C, were injected *via* the sample loop of the system, followed by regeneration of the surface by injection of 15 μl of 100 mM glycine (pH 2.3). Data were evaluated using BIAevaluation software (Pharmacia) and Kaleidagraph (Synergy Software, USA). Slopes of the association phase of linear sensograms were plotted against the corresponding total hapten concentrations, and the dissociation constant was calculated.

Fluorescence titration

A 2 ml sample of 20 mM Tris, 100 mM NaCl (pH 7.6), containing 0.1-0.5 μM active scFv Tras was placed in a cuvette with an integrated stirrer, equilibrated at 17 °C. Aliquots of concentrated traseolide stock (0.6 mM) were added and after ten minutes of equilibration a spectrum was recorded from 315 to 360 nm (excitation wavelength 280 nm) on a Timemaster™ fluorescence spectrometer (Photon Technology Int., Brunswick, NJ). Fluorescence emission spectra of scFv Tras fragments showed quenching of fluorescence upon formation of a complex of scFv

Tras with the hapten traseolide. The emission intensity at 335 nm was used for determining the degree of complexation as a function of traseolide concentration. The K_D value was determined by a direct fit of emission intensity *versus* hapten concentration (Jung & Plückthun, 1997).

Papain digestion and purification of Fab fragments

Mouse monoclonal antibody M02/05/01 (IgG1) was obtained from tissue culture of the relevant hybridoma cell culture medium and purified by Protein A affinity chromatography (MCA, Groningen). The following stock solutions in PBS were added to 10 ml of a M02/05/01 solution (4.4 mg/ml in PBS): 250 µl of 0.4 M L-cysteine-HCl (Sigma, C-1276) adjusted to pH 7.4 with 5 N NaOH, 500 µl of 0.04 M EDTA (Merck, 108418) and 440 µl of 1 mg/ml papain (Boehringer Mannheim, 108014). Papain digestion was allowed for three hours in an incubator shaker at 150 rpm at 37 °C. The reaction was stopped by addition of 500 µl of 0.15 M iodacetamide (Sigma, I-6125) to the reaction mixture.

Fab fragments were purified by ion-exchange chromatography. The digested antibody sample was dialyzed against running buffer (20 mM Tris-HCl (pH 8.25)) and subsequently applied onto a Q-Sepharose Fast Flow column (Pharmacia) equilibrated with running buffer at 1 ml/minute. A salt gradient was run in order to separate Fab fragments from non-digested antibodies and Fc fragments (gradient: 2 mM NaCl/ml in 20 mM Tris-HCl (pH 8.25) at 1 ml/minute). Fab fragments were eluted into two major protein peaks named Fab-1 and Fab-2, respectively. By iso-electric focusing (Fast-System, Pharmacia) the pI values of Fab-1 and Fab-2 were determined and found to be 7.4 and 6.9, respectively. In order to obtain highly pure Fab fractions, both samples were dialyzed against running buffer and subsequently applied onto a Mono-Q column (Pharmacia, 1 ml) as described above. A salt gradient was used to elute the Fab-1 and Fab-2 samples (gradient: 1 mM NaCl/ml at 1 ml/minute). One major Fab fraction was identified after purification of the Fab-1 sample. The Fab-2 sample, however, was separated into three peaks named Fab-2, Fab-2′ and Fab-2″, respectively. The four Fab fractions were collected separately and dialyzed against 50 mM Tris-HCl, 100 mM NaCl (pH 7.5). In an ELISA assay all four Fab fractions showed similar specific activities towards the traseolide molecule. Crystallization studies showed that best crystals were obtained with Fab fragments from the Fab-1 subclass. All further studies were done with the latter fragment.

Crystallization and data collection

Prismatic crystals were obtained using the hanging-drop vapor diffusion method at 20 °C. Drops consisting of 2 µl of a protein solution with or without hapten (5 mM hapten and 12 mg Fab per ml in 100 mM Tris, pH 7.0) were mixed with 2 µl of the well solution (18-19 % (w/v) PEG8000, 75-200 mM sodium acetate (pH 4.0)). Crystals belong to space group $P2_12_12$ with cell dimensions $a = 134.42$ Å, $b = 84.5$ Å and $c = 40.5$ Å. With one molecule in the asymmetric unit (assuming a molecular mass of 50 kDa) the specific protein volume is $V_m = 2.3$ Å^3/Da, which corresponds to a solvent content of 47 % (Matthews, 1968). The diffraction data were collected on a MAR-Research Imaging Plate (MAR, Hamburg, Germany) placed on a Rigaku RU200 rotating anode using the CuK_α radiation. Reflection intensities were indexed using MARXDS (Kabsch, 1988a) and merged/scaled using MARSCALE (Kabsch, 1988b). Details of the data processing are given in Table 2.

Structure determination and refinement

Both rotational and translational searches for the Fab fragment were performed with the program AMoRe (Navaza, 1994). Because of the flexibility of the elbow region, two rotation functions were performed, one for the V_H:V_L and one for the C_H1:C_L domains. The search model consisted of the variable domains of an anti-arsonate antibody (PDB file 2f19; Lascombe *et al.*, 1989) and the constant domains of an anti-oxazolone antibody (P.M. Alzari & S. Spinelli, unpublished results; Alzari *et al.*, 1990). The orientation of the variable and the constant domains were given by the two highest peaks in the corresponding rotation functions calculated with data between 10.0 and 3.5 Å. The resulting model had a *R*-factor of 0.40 and a correlation coefficient of 0.30. All maps were constructed using the CCP4 suite of programs (Collaborative Computational Project, Number 4, 1994), side-chains were substituted, inserted or deleted on the computer graphics according to the sequence of the authentic anti-traseolide Fab with the program Turbo-Frodo (Roussel & Cambillau, 1989). The refined structure of the Fab M02/05/01, complexed with traseolide, was obtained by cycles of model building alternated with refinement of the atomic coordinates by standard slow-cooling protocol using data between 12.0 and 2.6 Å (Brünger *et al.*, 1987). As the low-resolution data were employed in the refinement, a low-resolution bulk solvent correction, as implemented in the XPLOR program version 3.843 (Brünger, 1996) was applied. The behavior of the free *R*-factor (R_{free}) was monitored all along the refinement procedure (Brünger, 1992). Details of the refinement and model statistic are listed in Table 2.

Synthesis of musk odorant molecules

The commercial odorant traseolide (6-acetyl-1-isopropyl-2,3,3,5-tetramethylindane) is a musk type odorant, synthesized by Quest International (Naarden, the Netherlands). By using different starting materials, a series of traseolide analogs was synthesized at Quest International and the fragrance of these analogs was evaluated (Figure 1; Traas *et al.*, 1982).

In order to be able to raise antibodies against traseolide or use it in biological assays, a covalent hydrophilic linker was added to the hydrophobic odorant. This allowed attachment to a carrier protein and, at the same time, made the compound better soluble in aqueous solutions. The linker should preferably not interfere with the structurally important parts of the traseolide, so that antibodies could be obtained with structures resembling the olfactory receptor as closely as possible. From olfactive studies it was known that elongation of the R_1 chain did not have a significant influence on the fragrance (Quest International, the Netherlands). Therefore it was decided to introduce a carboxylic substituent in R_1 as reactive group for binding to the carrier proteins (the succinyl derivative of traseolide; Figure 1). The succinyl derivative of the original traseolide hapten was available from Unilever Research Vlaardingen (the Netherlands), while the succinyl derivatives of the other traseolide variants had to be synthesized from traseolide-alcohol 1-(2-hydroxy-3-methylpropyl)-4-methylbenzene (Traas *et al.*,

1982). First isobutylene, or 2-methyl-2-pentene respectively, was allowed to react with traseolide-alcohol in a [3 + 2]cycloaddition using $AlCl_3$ as Lewis base to form the traseolide-indane (Angle & Arnaiz, 1992). Secondly, the succinyl derivative was formed using the Friedel Crafts acylation conditions for musk odorants (Weber *et al*., 1955). The purity of the newly synthesized traseolide succinyl derivatives was checked by TLC, NMR and absorption spectroscopy (estimated purity: $T^{eth} \geqslant 95\%$ and $T^{-} \geqslant 85\%$ pure; data not shown). NMR spectra of traseolide indicated that the substituents in C_1 and C_2 are *in trans* (Figure 1) (R. Pepermans, unpublished results), and the absolute stereochemistry is deduced from the electron density map of Fab M02/05/01 complexed with the traseolide hapten. The (*S*,*S*) enantiomer is predominantly occupying the binding pocket, but it cannot be excluded that some (*R*,*R*) enantiomer is also present.

Protein Data Bank accession number

Coordinates of the complexed Fab M05/01/01 have been deposited in the Brookhaven Protein Data bank with accession number 1C12.

Acknowledgments

The authors thank J.A.M. Laan for synthesis of the succinyl derivative of traseolide, E.A. de Ron for production of monoclonal antibodies, W.J. Bos for sequencing of cDNA, L.F. Frenken for suggesting the Tras-P mutant, M. Scarsi for performing theoretical calculations of binding energies and preparing Figure 8, T. Carell of the ETH for the opportunity to work in his lab, and J. Maat and P. de Geus for initiating the project. This work was supported by the EC-grant BIOCT-920367.

References

Alzari, P. M., Spinelli, S., Mariuzza, R. A., Boulot, G., Poljak, R. J., Jarvis, J. M. & Milstein, C. (1990). Three-dimensional structure determination of an anti-2-phenyloxazolone antibody: the role of somatic mutation and heavy/light chain pairing in the maturation of an immune response. *EMBO J.* **9**, 3807-3814.

Amati, V., Werge, T. M., Cattaneo, A. & Tramontano, A. (1995). Identifying a putative common binding site shared by substance P receptor and an anti-substance P monoclonal antibody. *Protein Eng.* **8**, 403-408.

Anchin, J. M. & Linthicum, D. S. (1993). Variable region sequence and characterization of monoclonal antibodies to a N,N′,N″-trisubstituted guanidine high potency sweetener. *Mol. Immunol.* **30**, 1463-1471.

Anchin, J. M., Nagarajan, S., Carter, J., Kellog, M. S., DuBois, G. E. & Linthicum, D. S. (1997). Recognition of superpotent sweetener ligands by a library of monoclonal antibodies. *J. Mol. Recogn.* **10**, 235-242.

Angle, S. R. & Arnaiz, D. O. (1992). Formal [3 + 2] cycloaddition of benzylic cations with alkenes. *J. Org. Chem.* **57**, 5937-5947.

Arevalo, J. H., Stura, E. A., Taussig, M. J. & Wilson, I. A. (1993). Three-dimensional structure of an anti-steroid Fab′ and progesterone-Fab′ complex. *J. Mol. Biol.* **231**, 103-118.

Arevalo, J. H., Hassig, C. A., Stura, E. A., Sims, M. J., Taussig, M. J. & Wilson, I. A. (1994). Structural analysis of antibody specificity. Detailed comparison of five Fab′-steroid complexes. *J. Mol. Biol.* **241**, 663-690.

Ayala, M., Balint, R. F., Fernández-de-Cossío, M. E., Canaán-Haden, L., Larrick, J. W. & Gavilondo, J. V. (1995). Variable region sequence modulates periplasmic export of a single-chain Fv antibody fragment in *Escherichia coli*. *Biotechniques,* **18**, 832-842.

Bergner, A., Bauer, M., Brandstetter, H., Stürzebecher, J. & Bode, W. (1995). The X-ray crystal structure of thrombin in complex with N_{α}-2-naphthylsulfonyl-L-3-amidino-phenylalanyl-4-methylpiperidide: the beneficial effect of filling out an empty cavity. *J. Enzyme Inhib.* **9**, 101-110.

Bianchet, M. A., Bains, G., Pelosi, P., Pevsner, J., Snyder, S. H., Monaco, H. L. & Amzel, L. M. (1996). The three-dimensional structure of bovine odorant binding protein and its mechanism of odor recognition. *Nature Struct. Biol.* **3**, 934-939.

Bode, W. (1979). The transition of bovine trypsinogen to a trypsin-like state upon strong ligand binding. *J. Mol. Biol.* **127**, 357-374.

Brünger, A. T. (1992). Free *R* value: a novel statistical quantity for assessing the accuracy of crystal structures. *Nature,* **355**, 472-475.

Brünger, A. T. (1996). *XPLOR Version 3.843 Manual*, Yale University Press, New Haven, CT.

Brünger, A. T., Kuriyan, J. & Karplus, M. (1987). Crystallographic *R* factor refinement by molecular dynamics. *Science,* **235**, 458-460.

Buchner, J. & Rudolph, R. (1991). Renaturation, purification and characterization of recombinant Fab-fragments produced in *Escherichia coli*. *Biotechnology,* **9**, 157-162.

Buck, L. (1996). Information coding in the vertebrate olfactory system. *Annu. Rev. Neurosci.* **19**, 517-544.

Buck, L. & Axel, R. (1991). A novel multigene family may encode odorant receptors: a molecular basis for odorant recognition. *Cell,* **65**, 175-187.

Clark, M., Cramer, R. D., III & Van Opdenbosch, N. (1989). Validation of the General Purpose Tripos 5.2 Force Field. *J. Comp. Chem.* **10**, 982-1012.

Collaborative Computational Project Number 4 (1994). The CCP4 suite: programs for protein crystallography. *Acta Crystallog. sect. D,* **50**, 760-763.

Cook, E. C. & Drayer, D. E. (1988). Antibodies, a rich source of novel chemical agents for pharmacological studies. *Trends Pharmacol. Sci.* **9**, 373-375.

Döring, E., Stigler, R., Grütz, G., Von Baehr, R. & Schneider-Mergener, J. (1994). Identification and characterization of a TNFα antagonist derived from a monoclonal antibody. *Mol. Immunol.* **31**, 1059-1067.

Dougan, D. A., Malby, R. L., Gruen, L. C., Kortt, A. A. & Hudson, P. J. (1998). Effects of substitutions in the binding surface of an antibody on antigen affinity. *Protein Eng.* **11**, 65-74.

Ducancel, F., Mérienne, K., Fromen-Romano, C., Trémeau, O., Pillet, L., Drevet, P., Zinn-Justin, S., Boulain, J. C. & Ménez, A. (1996). Mimicry between receptors and antibodies. Identification of snake toxin determinants recognized by the acetylcholine receptor and an acetylcholine receptor-mimicking monoclonal antibody. *J. Biol. Chem.* **271**, 31345-31353.

Fersht, A. R. (1985). *Enzyme Structure and Mechanism*, 2nd edit., pp. 293-311, W. H. Freeman and Company, New York.

Freund, C., Ross, A., Guth, B., Plückthun, A. & Holak, T. A. (1993). Characterization of the linker peptide of the single-chain Fv fragment of an antibody by NMR spectroscopy. *FEBS Letters,* **320**, 97-100.

Friguet, B., Chaffotte, A. F., Djavadi-Ohaniance, L. & Goldberg, M. E. (1985). Measurements of the true affinity constant in solution of antigen-antibody complexes by enzyme-linked immunosorbent assay. *J. Immun. Methods,* **77**, 305-319.

Ge, L., Knappik, A., Pack, P., Freund, C. & Plückthun, A. (1995). Expressing antibodies in *Escherichia coli*. In *Antibody Engineering* (Borrebaeck, C. A. K., ed.), 2nd edit., pp. 229-266, Oxford Univeristy Press, Oxford.

Gill, S. C. & von Hippel, P. H. (1989). Calculation of protein extinction coefficients from amino acid sequence data. *Anal. Biochem.* **182**, 319-326.

Hammarberg, B., Moks, T., Tally, M., Elmblad, A., Holmgren, E., Murby, M., Nilsson, B., Josephson, S. & Uhlen, M. (1990). Differential stability of recombinant human insulin-like growth factor II in *Escherichia coli* and *Staphylococcus aureus*. *J. Biotechnol.* **14**, 423-437.

Hanes, J., Jermutus, L., Weber-Bornhauser, S., Bosshard, H. R. & Plückthun, A. (1998). Ribosome display efficiently selects and evolves high-affinity antibodies *in vitro* from immune libraries. *Proc. Natl Acad. Sci. USA,* **95**, 14130-14135.

Jackson, S. E., Moracci, M., ElMasry, N., Johnson, C. M. & Fersht, A. R. (1993). Effect of cavity-creating mutations in the hydrophobic core of chymotrypsin inhibitor 2. *Biochemistry,* **32**, 11259-11299.

Jeffrey, P. D., Strong, R. K., Sieker, L. C., Chang, C. Y. Y., Campbell, R. L., Petsko, G. A., Haber, E., Margolies, M. N. & Sheriff, S. (1993). 26-10 Fab-digoxin complex: affinity and specificity due to surface complementarity. *Proc. Natl Acad. Sci. USA,* **90**, 10310-10314.

Jung, S. & Plückthun, A. (1997). Improving *in vivo* folding and stability of a single-chain Fv antibody fragment by loop grafting. *Protein Eng.* **10**, 959-966.

Kabat, E. A., Wu, T. T., Perry, H. M., Gottesman, K. S. & Foeller, C. (1991). *Sequences of proteins of Immunological Interest*, 5th edit., U.S. Department of Health and Human Services, Public Health Service, National Institutes of Health, Bethesda, MD.

Kabsch, W. (1988a). Automatic indexing of rotation diffraction patterns. *J. Appl. Crystallog.* **21**, 67-71.

Kabsch, W. (1988b). Evaluation of single crystal X-ray diffraction data from a position sensitive detector. *J. Appl. Crystallog.* **21**, 916-924.

Karlsson, R. (1994). Real-time competitive kinetic analysis of interactions between low-molecular-weight ligands in solution and surface-immobilized receptors. *Anal. Biochem.* **221**, 142-151.

Kevekordes, S., Mersch-Sundermann, V., Diez, M., Bolten, C. & Dunkelberg, H. (1998). Genotoxicity of polycyclic musk fragrances in the sister-chromatid exchange test. *Anticancer Res.* **18**, 449-452.

Kiefer, H., Krieger, J., Olszewski, J. D., von Heijne, G., Prestwich, G. D. & Breer, H. (1996). Expression of an olfactory receptor in *Escherichia coli*: purification, reconstitution and ligand binding. *Biochemistry,* **35**, 16077-16084.

Knappik, A. & Plückthun, A. (1994). An improved affinity tag based on the FLAG® peptide for the detection and purification of recombinant antibody fragments. *Biotechniques,* **17**, 754-761.

Krautwurst, D., Yau, K. W. & Reed, R. R. (1998). Identification of ligands for olfactory receptors by functional expression of a receptor library. *Cell,* **95**, 917-926.

Kussie, P. H., Albright, G. & Linthicum, D. S. (1989). Production and characterization of monoclonal idiotypes and anti-idiotypes for small ligands. *Methods Enzymol.* **178**, 49-63.

Laemmli, U. K. (1970). Cleavage of structural proteins during the assembly of the head of bacteriophage T4. *Nature,* **227**, 680-685.

Langedijk, A. C., Honegger, A., Maat, J., Planta, R. J., van Schaik, R. C. & Plückthun, A. (1998). The nature of antibody heavy chain residue H6 strongly influences the stability of a V_H domain lacking the disulfide bridge. *J. Mol. Biol.* **283**, 95-110.

Lascombe, M. B., Alzari, P. M., Boulot, G., Saludjian, P., Tougard, M., Berek, C., Haba, S., Rosen, E. M., Nisonoff, A. & Poljak, R. J. (1989). Three-dimensional structure of Fab R19.9, a monoclonal murine antibody specific for the p-azobenzenearsonate group. *Proc. Natl Acad. Sci. USA,* **86**, 607-611.

Lindner, P., Bauer, K., Krebber, A., Nieba, L., Kremmer, E., Krebber, C., Honegger, A., Klinger, B., Mocikat, R. & Plückthun, A. (1997). Specific detection of His-tagged proteins with recombinant anti-His tag scFv-phosphatase or scFv-phage fusions. *Biotechniques,* **22**, 140-149.

Malby, R. L., Tulip, W. R., Harley, V. R., KcKimm-Breschkin, J. L., Laver, W. G., Webster, R. G. & Colman, P. M. (1994). The structure of a complex between the NC10 antibody and influenza virus neuraminidase and comparison with the overlapping binding site of the NC41 antibody. *Structure,* **2**, 733-746.

Mariuzza, R. A., Poljak, R. J. & Schwarz, F. P. (1994). The energetics of antigen-antibody binding. *Res. Immunol.* **145**, 70-72.

Markiewcz, P. (1991). Computer software for molecular biology. *Biotechniques,* **10**, 756-763.

Matthews, B. W. (1968). Solvent content of protein crystals. *J. Mol. Biol.* **33**, 491-497.

Mombaerts, P. (1996). Targeting olfaction. *Curr. Opin. Neurobiol.* **6**, 481-486.

Navaza, J. (1994). AMoRe: an automated package for molecular replacement. *Acta Crystallog. sect. A,* **50**, 157-163.

Nekrasova, E., Sosinskaya, A., Natochin, M., Lancet, D. & Gat, U. (1996). Overexpression, solubilization and purification of rat and human olfactory receptors. *Eur. J. Biochem.* **238**, 28-37.

Nieba, L., Krebber, A. & Plückthun, A. (1996). Competition BIAcore for measuring true affinities: large differences from values determined from binding kinetics. *Anal. Biochem.* **234**, 155-165.

Ohloff, G. (1990). Animalische Drogen ab Riechstoffe. In *Riechstoffe und Geruchsinn. Die Molekulare Welt der Düfte*, pp. 195-199, Springer-Verlag, Berlin and Heidelberg.

Omelyanenko, V. G., Jiskoot, W. & Herron, J. N. (1993). Role of electrostatic interactions in the binding of fluorescein by anti-fluorescein antibody 4-4-20. *Biochemistry,* **32**, 10423-10429.

Pelosi, P. (1994). Odorant-binding proteins. *Crit. Rev. Biochem. Mol. Biol.* **29**, 199-228.

Prickett, K. S., Amberg, D. C. & Hopp, T. P. (1989). A calcium-dependent antibody for identification and

purification of recombinant proteins. *Biotechniques,* **7**, 580-589.
Privalov, P. L. (1979). Stability of proteins: small globular proteins. *Advan. Protein Chem.* **33**, 167-236.
Proba, K., Honegger, A. & Plückthun, A. (1997). A natural antibody missing a cysteine in V_H: consequences for thermodynamic stability and folding. *J. Mol. Biol.* **265**, 161-172.
Raming, K., Krieger, J., Strotmann, J., Boekhoff, I., Kubick, S., Baumstark, C. & Breer, H. (1993). Cloning and expression of odorant receptors. *Nature,* **361**, 353-356.
Recinos, A., III, Silvey, K. J., Ow, D. J., Jensen, R. H. & Stanker, L. H. (1994). Sequences of cDNAs encoding immunoglobulin heavy- and light-chain variable regions from two anti-dioxin monoclonal antibodies. *Gene,* **149**, 385-386.
Roussel, A. & Cambillau, C. (1989). Editors of Silicon Graphics Geometry Partner Directory (Fall 1989), pp. 77-78, Silicon Graphics, Mountain View, CA.
Sawutz, D. G., Sylvestre, D. & Homcy, C. J. (1985). Characterization of monoclonal antibodies to the β-adrenergic antagonist alprenolol as models of the receptor binding site. *J. Immunol.* **135**, 2713-2718.
Schild, D. & Restrepo, D. (1998). Transduction mechanisms in vertebrate olfactory receptor cells. *Physiol. Rev.* **78**, 429-466.
Schmitter, D., Poch, O., Zeder, G., Heinrich, G. F., Kocher, H. P., Quesniaux, V. F. J. & Van Regenmortel, M. H. V. (1990). Analysis of the structural diversity of monoclonal antibodies to cyclosporine. *Mol. Immunol.* **27**, 1029-1038.
Schuck, P. (1997). Use of surface plasmon resonance to probe the equilibrium and dynamic aspects of interactions between biological macromolecules. *Annu. Rev. Biophys. Biomol. Struct.* **26**, 541-566.
Serrano, L., Kellis, J. T., Cann, P., Matouschek, A. & Fersht, A. R. (1992). The folding of an enzyme. II. Substructure of barnase and the contribution of different interactions to protein stability. *J. Mol. Biol.* **224**, 783-804.
Solin, M. L., Kaartinen, M. & Mäkelä, O. (1992). The same few V genes account for a majority of oxazolone antibodies in most mouse strains. *Mol. Immunol.* **29**, 1357-1362.
Spinelli, S., Ramoni, R., Grolli, S., Bonicel, J., Cambillau, C. & Tegoni, M. (1998). The structure of monomeric porcine odorant binding protein sheds light on the domain swapping mechanism. *Biochemistry,* **37**, 7913-7918.
Studier, F. W. & Moffatt, B. A. (1986). Use of bacteriophage T7 RNA polymerase to direct selective high-level expression of cloned genes. *J. Mol. Biol.* **189**, 113-130.
Summers, R. G., Harris, C. R. & Knowles, J. R. (1989). A conservative amino acid substitution, arginine for lysine, abolishes export of a hybrid protein in *Escherichia coli*. Implications for the mechanism of protein secretion. *J. Biol. Chem.* **264**, 20082-20088.
Tegoni, M., Ramoni, R., Bignetti, E., Spinelli, S. & Cambillau, C. (1996). Domain swapping creates a third putative combining site in bovine odorant binding protein dimer. *Nature Struct. Biol.* **3**, 863-867.
Tovay, E. R. & Baldo, B. A. (1987). Comparison of semi-dry and conventional tank-buffer electrotransfer of proteins from polyacrylamide gels to nitrocellulose membranes. *Electrophoresis,* **8**, 384-387.
Traas, P. C., Renes, H. & Boelens, H. (1982). Novel acyl-polyalkylindan compounds and the use thereof as a base for perfume, as well as perfume compositions, US patent 4,352,748.
Trinh, C. H., Hemmington, S. D., Verhoeyen, M. E. & Phillips, S. E. V. (1997). Antibody fragment Fv4155 bound to two closely related steroid hormones: the structural basis of fine specificity. *Structure,* **5**, 937-948.
Volkin, D. B. & Klibanov, A. M. (1989). Minimizing protein inactivation. In *Protein Function: A Practical Approach* (Creighton, T. E., ed.), pp. 1-24, IRL Press, Oxford.
von Heijne, G. (1986). The distribution of positively charged residues in bacterial inner membrane proteins correlates with the trans-membrane topology. *EMBO J.* **5**, 3021-3027.
Walbaum, H. (1906). Das natürliche Moschusaroma. *J. Prakt. Chem.* **73**, 488-493.
Weber, S. H., Spoelstra, D. B. & Polak, E. H. (1955). New musk odorants. The structure of tert. amylated p-cymene. A new synthesis of polyalkylindans. *Recueil,* **74**, 1179-1196.
Webster, D. M., Henry, A. H. & Rees, A. R. (1994). Antibody-antigen interactions. *Curr. Opin. Struct. Biol.* **4**, 123-129.
Witholt, B., Boekhout, M., Brock, M., Kingma, H., van Heerikhuizen, H. & de Leij, L. (1976). An efficient and reproducible procedure for the formation of spheroplasts from variously grown *Escherichia coli*. *Anal. Biochem.* **74**, 160-170.
Wysocki, L. J., Gridley, T., Huang, S., Grandea, G. & Gefter, M. L. (1987). Single germline V_H and V_K genes encode predominating antibody variable regions elicited in strain A mice by immunization with *p*-azophenylarsonate. *J. Exp. Med.* **166**, 1-11.
Yanisch-Perron, C., Vieira, J. & Messing, J. (1985). Improved M13 phage cloning vectors and host strains: nucleotide sequences of the M13mp18 and pUC19 vectors. *Gene,* **33**, 103-119.
Zhao, H., Ivic, L., Otaki, J. M., Hashimoto, M., Mikoshiba, K. & Firestine, S. (1998). Functional expression of a mammalian odorant receptor. *Science,* **279**, 237-242.

Edited by R. Huber

(Received 12 April 1999; received in revised form 9 August 1999; accepted 9 August 1999)